

Remote Sensing for Mapping of India's Irrigated Farmland

Chandra Kanthi¹ & Manisha Mishrai²

¹ Remote Sensing Applications Centre, Uttar Pradesh, Lucknow-226021, India, Email: chandrakantpandey.pandey@gmail.com

² Remote Sensing Applications Centre, Uttar Pradesh, Lucknow-226021, India, Email: manishamishrai1012@gmail.com)

Abstract

This study was conducted to calculate the irrigated area in the Hamirpur district of Uttar Pradesh using data collected by the Landsat-8 satellite. This research retrieved the irrigated area using Normalized Difference Vegetation Index (NDVI) and a Least Squares Thresholding (LST) based technique. Chander et al. (2003) report that TIR band data from both spring and summer may be converted to temperature (Ts). After calculating the NDVI in the spring and summer, the pictures were processed using a differencing and thresholding technique to isolate regions that had undergone substantial seasonal change. A logical expression (NDVI 0.30) AND (T 293° K) was used to NDVI and LST pictures in the identified substantially modified region (crop region) to distinguish irrigated agricultural areas from non irrigated cropland areas. The estimated irrigated area was validated against data from the district irrigation department, and we discovered that it was 98% accurate.

Keywords: *Luminance and Spectral Flux, Least Squares Error, and Landsat Feature Validation and Characterization.*

1. Introduction

With a rapidly expanding global population comes an urgent need to boost agricultural food production (1). In arid and semi-arid areas, agriculture accounts for the vast majority of water withdrawals and has a significant impact on the water cycle due to its reliance on groundwater and the

diversion of surface water(1). The water supply on Earth may seem plentiful, but only around 1% of it is really drinkable since the other 70% is needed to irrigate crops(2). Satellite remote sensing data has been proved to be valuable in a number of studies for determining things like total irrigated area, area under various crops, crop condition, agricultural yield, and so on. The most widely used method for identifying irrigated crops nowadays is...

strategies include principal component analysis, simple ratio analysis, normalized difference vegetation index analysis, normalized difference wetness index analysis, green vegetation index analysis, and NDVI analysis.

(14), (15), (16). Toomanian had looked on comparing NOAA AVHRR NDVI photos to Landsat images to estimate the irrigated area(17).

Large regions may be evaluated with ease using remotely sensed data, and a lot of work has gone into characterizing vegetation using satellite imagery. Spectral reflectance and plant traits are related in fundamental ways. Because of these connections, spectral transformations may be used to specify plant biophysical characteristics.

Evidence suggests that plant canopy factors, such as ET(18), (19), and (20), (21) are linked to the normalized differential vegetation index.

This study uses satellite imagery to decipher the connections between soil moisture, surface temperature (ST), and vegetation indices (such ST/NDVI). When considering climate, hydrology, and ecology, soil moisture is one of the most crucial terrestrial environmental variables(22). Ts is inversely associated with NDVI(23) and decreases as soil moisture increases, as discovered by Samuel N. Gowarda.

The biophysical mechanisms that regulate the water and energy balances at the land's surface may be understood in large part via the LST and surface emissivity. Boundary conditions for models of air movement and water movement in the soils may be derived from knowledge of how the fluxes of energy and water fluctuate at the local and regional levels (29). Thermal infrared (TIR) AVHRR data was first exploited by Vidal.

to learn more about the irrigation system's water efficiency (30). It is determined from the research of Vidal and Perrier (1990) that land surface temperature (ST) has the potential to be a useful indication of watering needs.

Irrigated regions have higher NDVI values but lower Ts values than rainfed areas because to their higher moisture content. Therefore, a combination of LST and NDVI would be a great tool for locating watered regions. It has been noted that the ST variation in woods is

comparable to that in the spring picture of irrigated farmland. Since forest, grassland, and permanent trees remain evergreen in both spring and summer without any noticeable phenological shift, it was required to separate them from the irrigated fields by utilizing a differencing and thresholding approach using pictures from both seasons.

district is about 4,121.9 km².

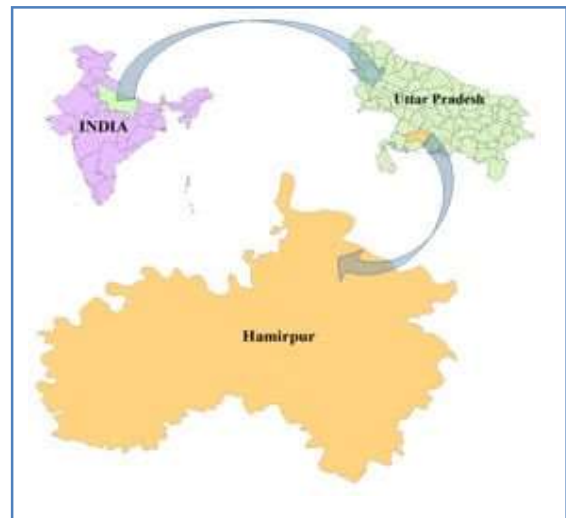


Figure 1: Location Map of the Study Area.

2. Data & Methods

2.1 Study Area:

Hamirpur is located at 25.95°N latitude and 80.15°E longitude. It has an average elevation of 80 metres. The district is bounded by districts Jalaun , Kanpur and Fatehpur in the North, Banda in the East,

Mahoba in South and Districts of Jhansi and Jalaun on the West. As per 2001 census, the district has a population of 1043724. It has 4 tehsils,7 blocks and 647 villages. Average maximum and minimum temperatures are 43.0o C and 3.0o C respectively. Total area covered by Hamirpur

2.2 Data Used

The Landsat Satellite imagery December

May 2014 (Landsat-8 OLI_TIRS) were used in present study area. The detail of the satellite images is given below:

Satellite digital data: Landsat

- 8 Bands : Red, Near Infrared

(NIR) Spatial resolution : 30m

Software Used: QGIS, Microsoft Excel

2.3 Methodology

2.4 In this research, we used an Earth Explorer Landsat-8 satellite picture to derive the NDVI. Images were resampled to 30-m pixels using the closest neighbor technique after being adjusted to remove atmospheric influences. The thermal band was converted to the temperature (ST) for both the spring and summer images using the method described by Chander et al. (2003); the NDVI was calculated for both the spring and summer times of the year; and finally, the Differencing and thresholding method was applied to the NDVI of both the spring and summer images in order to distinguish between areas with significant phenological change (such as irrigated land and rainfed cropland where $NDVI > 0.1$) and those

2.5 According to a preliminary evaluation of the research region, the NDVI is higher in irrigated areas while having the same climate as rainfed areas, which means that the LST in irrigated areas is often 2 to 4 degrees Celsius lower than in rainfed areas.

In the identified significantly changed area, a logical expression ($NDVI \geq 0.30$) AND ($T \leq 293^{\circ}K$) was applied on

NDVI and LST images to differentiate the irrigated cropland areas from the non irrigated croplands. The thresholds of NDVI and LST may be slightly different from scene to scene and from spring to summer time.

Figure 2: Flow chart of methodology.

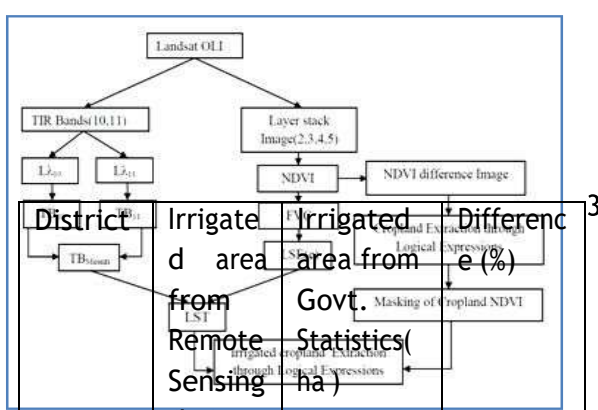
3. Results and Discussion

According to our findings, in 2014, roughly 91441.98 hectares were irrigated throughout the winter in Hamirpur District. Only 28.14 percent of the total agricultural land is irrigated, out of a total of 32,493 hectares in agriculture (including irrigated and rain-fed) in 2014. The rivers Yamuna, Betwa, Dashan, Barma, Ken, Chandrawal, and Pandwaha all contribute to the construction of canals that are used for irrigation. The geographical distribution of irrigated land in the Hamirpur District is shown in Fig. 3. The southern half of the land seems to be more heavily irrigated, while the eastern and western parts of the territory exhibited modest irrigating, and the middle part of the area appears to be rain-fed. Using information from the District Irrigation Department, we were able to verify that our estimates of the irrigated area were, on average, 98% accurate (Sankhikiya Patrika, Hamirpur, 2014). The accuracy of irrigated area estimates may be improved through field verification.

Identifying Crops Grown with Irrigation...

and cross checking the results, but this part is not carried out in the study area due to lack of resources.

Table 1: Comparison of Remote sensing & Govt. data.



σ = Boltzman universal constant (1.38 $\times 10^{-23}$ J/K)
 h = Planck universal constant (6.626 $\times 10^{-34}$ J s)
 c = velocity of light (2.998 $\times 10^8$ m/s)

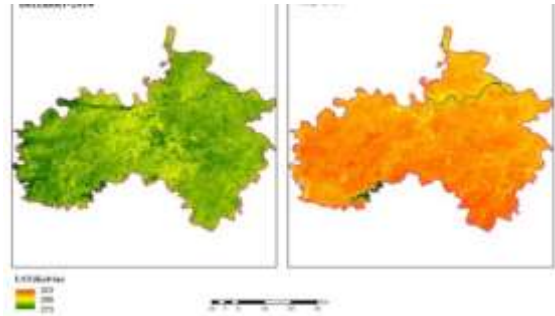


Figure 4: Land Surface Temperature of the study area.

3.1.1 Brightness

temperature(TB)- Brightness temperature is the microwave radiation radiance traveling upward from the top of Earth's atmosphere. Calibration process has been done for converting thermal DN values of thermal bands of TIR to TB. For finding brightness temperature of an area the Top of Atmospheric (TOA) spectral radiance of (L_λ) was needed. TB for both the TIRs bands was calculated by using the following formula. (26)

$$TB = K_2 / \ln((K_1 / L_\lambda) + 1) \quad (ii)$$

Where,

K_1 and K_2 are thermal conversion constant and it differ for both TIR bands (table 2)

L_λ - Top of Atmospheric spectral radiance.

The value of Top of Atmospheric spectral radiance (L_λ) was determined by multiplying M_L factor of TIR bands with its corresponding thermal infrared band and adding additive rescaling factor with it (27).

$$L_\lambda = M_L * Q_{cal} + A_L \quad (iii)$$

Figure 3: Distribution of spring irrigated cropland in the study area.

3.1 Retrieval of Land Surface Temperature-The

brightness temperatures(TB) from OLI thermal band (10&11) were averaged then used to calculate the land surface temperature using the Sobrino equation(25). Land Surface temperature in present study area ranges 281.780K to 294.990K in the month of December and 301.700K to 3230K in the month of May.

$$LST = TB / 1 + (\lambda * TB / \rho) * \ln(\epsilon) \quad (i)$$

Where,

$$\rho = h * c / \sigma \{ 1.438 \times 10^{-2} \text{ m K} \}$$

λ = wavelength of emitted radiance (= 11.5 μm)

Where,

L_{λ} - Top of Atmospheric Radiance in watts/($m^2 \cdot sr \cdot \mu m$)

M_L - Band specific multiplicative rescaling factor

(radiance_mult_band_10/11)

Chandra Kant & Manisha Mishra

Q_{cal} - for band 10/ 11 image.

A_L - Band specific additive rescaling factor

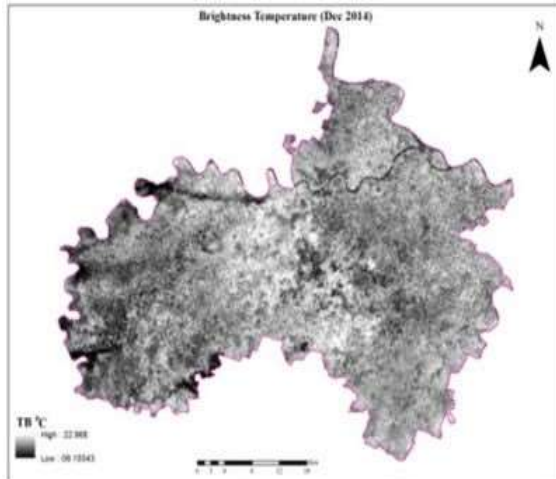


Figure 5: Distribution of spring irrigated cropland in the study area.

3.1.2 Land surface emissivity: It is necessary to be calculate the LSE of the region to find out Land surface temperature .

LSE was estimated using NDVI threshold method. (28) $LSE(\epsilon) = 0.004 \cdot FVC + 0.986$ (iv)

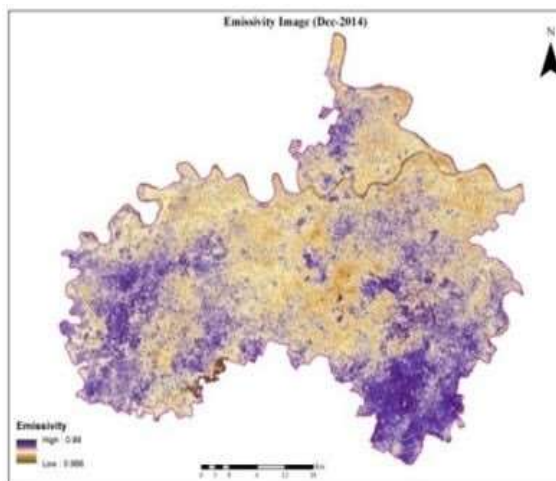


Figure 6: Land Surface Emissivity of the study area.

Fractional vegetation cover (FVC) was calculated as suggested by Sobrino(28) using NDVI.

3.2 NDVI Calculation

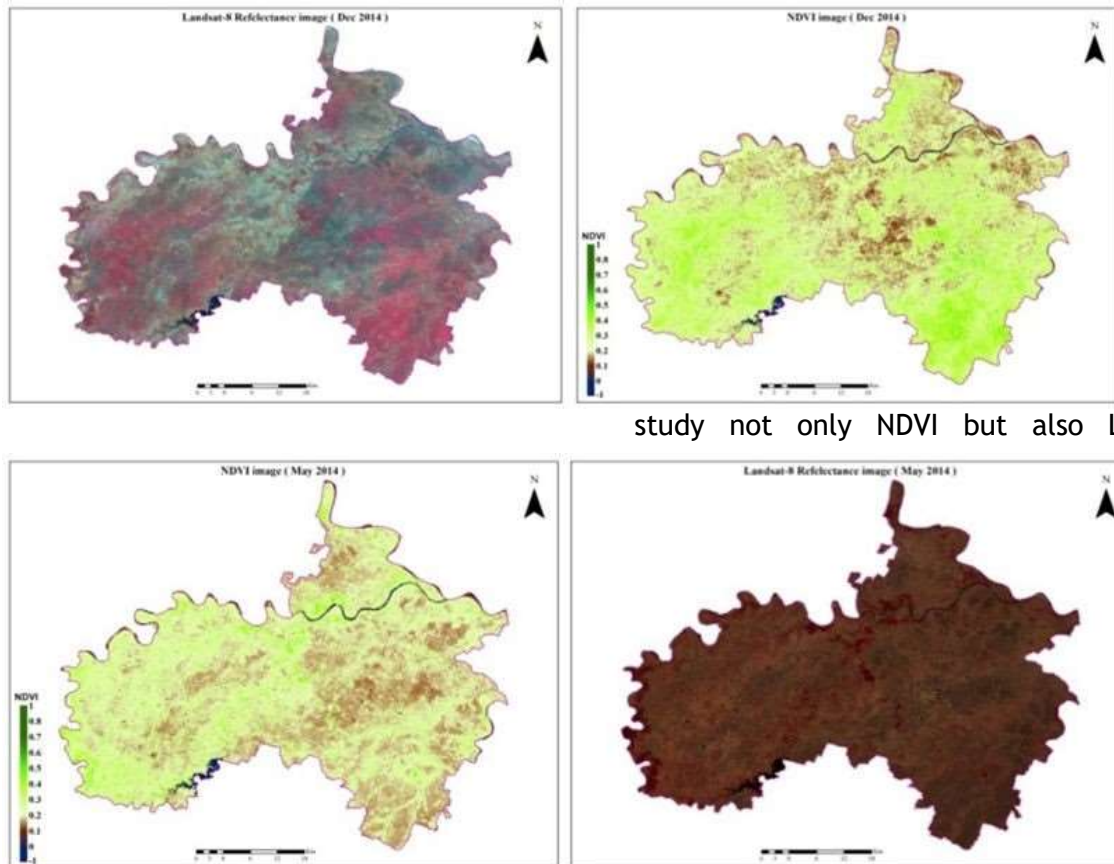
OLI bands 2, 3, 4 and 5 were layer stacked and converted it to reflectance values then NDVI was calculated using Q-GIS software for spring and summer of the year. The output value of NDVI ranged between -0.15 and 0.59 in the month of

December and -0.29 to 0.69 in the month of may in 2014. Differencing and thresholding method have been used on the NDVI of spring and summer season satellite images to separate the significantly changed areas (for example, irrigated cropland and rain fed cropland where $(\Delta NDVI > 0.1)$) from the non-significant phenological change land cover such as forests, grassland, or

permanent trees and water (e.g. $\Delta\text{NDVI} < 0.1$).

Irrigated Cropland Identification...

and facile to obtain Landsat data. In this



study not only NDVI but also LST

Figure 7: NDVI images of the study study area.

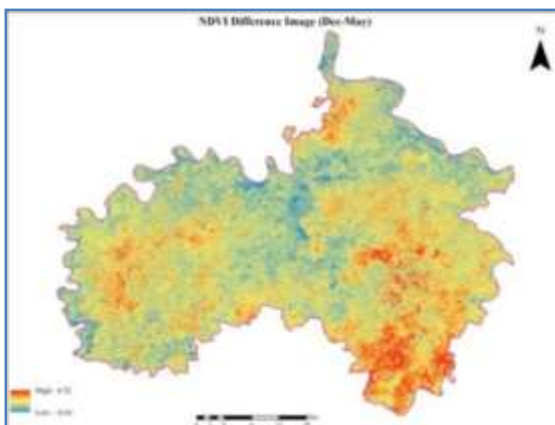


Figure 8: NDVI Deference image of the studyarea.

4. Conclusions

The study indicates that high temporal & spatial resolution remote sensing data that is Landsat data can improve monitoring of irrigation in a large region. Furthermore, it is free-cost, convenient

deriving from Landsat data is used to determine the irrigated area, and the result express that the combination of both is effective to obtain the useful information about crop developing conditions and canopy temperatures, both of which are relative to soil moisture.

For bettering the accuracy of irrigated area, we recommend that a detailed investigation of crop calendar of different locations in the present study area should be achieve. And experiments to determine NDVI and LST thresholds of locations with various climates, topography and crop calendars which may impact irrigation system & soil moisture are recommended in the future after successfully bring about more accurate irrigation area.

Photogrammetric Engineering and Remote Sensing.

Reference

- 1.1. calculating irrigation needs by inverse biophysical modeling and vegetation indicators. Shannon Franks, Marc L. Imhoff, and Lahouari Bounoua. Date of publication:2010, AGARSS, page 1823.
2. Second, the current state of water and agricultural progress. International Water Management Institute; D. Molden, K. Frenken, R. Barker, et al.
3. Third, using Landsat pictures to determine what kinds of irrigated crops are being grown and how many acres they take up. HC., KE. Kenneth, and L. HC. Pages 1479-1490 in the 1984 issue of
4. Using satellite imagery, compile an inventory of farmland in the Krishnarajasagar project's control region. Mohan Kumar, A., Nageswar Rao, P.P. Journal of Remote Sensing, Volume 15 Number 6, Pages 1295-1305, 1994.
5. The relationship between yield and yield characteristics and the spectral responses of a rice crop. Reference: Singh PNK, TP Sahai, and MS Patel. "International Journal of Remote Sensing," vol. 6, no. 6, pages 657-664, 1985.
6. Short-wave vegetation index images are used to provide a phenological description of Iberian vegetation. Lloyd, you get a. 1989, vol.10, no.4, pp.827-833 in the International Journal of Remote Sensing.
7. Potential and actual agricultural production estimation by remote sensing. Remote Sensing of Environment, Volume 13, Issue 4, Pages 301-311, 1983, J.K. Hatfield.
8. Eight, the normalized difference vegetation index is sensitive to factors including soil albedo, pixel size, and canopy cover at the sub-pixel level. Remote Sensing of Environment, Volume 32, Issue 2, Pages 169-187, 1990, by MF., Jasinski.
9. Using satellite data to enhance ground sampling and estimate crop yields. International Journal of Remote Sensing. Vol. 17, No. 6. Pages 945-956. Murthy CS, S. Thiruvengadachari, P.V. Raju,

- and S. Jonna.
10. Semiarid region irrigation patterns in India as seen from satellite. Photogrammetric Engineering and Remote Sensing, Volume 47, Issues 1493-1499, 1981, by S. Thiruvengadachari.
 11. Eleven. Using Landsat images to classify irrigated crops and calculate acreage. Photogrammetric Engineering and Remote Sensing, 50, 1479-1490, 1984, Kolm, K.E., and H.L. Case.
 12. 12 Seasonal digital change detection analysis of IRS-LISS 2 data for crop monitoring of irrigated crops. International Journal of Remote Sensing, Volume 16 (1995), Pages 633-640, Manavalan, P., K. Kesavasamy, and S. Adiga.
 13. 13. Seasonal image classification for irrigated agricultural monitoring in a salt-affected region in Australia. Published in 2001 in volume 22 of the International Journal of Remote Sensing, pages 717-726, the work of Abuzar, McAllister, and Morris.
 14. Estimating the Area of Irrigated Crops in La Mancha, Spain, Using Landsat TM Imagery. Irrigated crop area estimate. Beltran, C.M., and A.C. Belmonte. 2001. Photogrammetric Engineering and Remote Sensing. 67.
 15. Identifying Crops Grown with Irrigation...
 16. 15 Using multi-temporal MODIS photos to map paddy rice farming in southern China. 2005, Remote Sensing of Environment, volume 95, pages 480-492; Xiao, X.; Boles, S.; Liu, J.; Zhuang, D.; Frohling, S.; Li, C.; Salas, W.; Moore III, B.
 17. Low-cost Earth Observation satellite mapping of irrigated land in Mediterranean basins. In 2008, volume 64 of Computers and Electronics in Agriculture was published with contributions by T.K. Alexandridis, G.C. Zalidis, and N.G. Silleos.
 18. Zayandeh River Basin, Isfahan, Iran: Determining Irrigated Area Using NOAA-Landsat Upscaling Methods. Akbary, M., Toomanian, N., and A.S.M. Gieske. Volume 25, issue 9 (September 2004), pages 4945-4960, International Journal of Remote Sensing.
 19. Wheat Landsat estimations of the leaf area index and the effects on evaporation and crop simulation. 1979, Agron. J. 71, pages 336-342; Wiegand, C. L., A. J. Richardson, and E. T. Kanemasu.
 20. 19 Combinations of red and photographic infrared light for linear vegetation monitoring. C. Tucker.
 21. J. 1979, Vol. 8, No. 2, Pp. 127-150, Remote Sens. Environ.
 22. Spectral measurements for evaluating grassland biophysical parameters. Weiser, R. L., G. Asrar, G. P. Miller, and E. T. Kanemasu published their findings in 1986's Remote Sensing of the Environment, volume 20.
 23. 21. The role of vegetation in the dryland evaporative flux in a humid environment. To cite this article: Ritchie, J. T., and E. Burnett. 1971. Agron. J., 63, 56-62.

24. 22. Science goals, methodologies, and implementation of remote sensing of the terrestrial biosphere and biogeochemistry in the EOS era. *Global and Planetary Change*, Volume 7 (1993), Pages 279-297, Sellers, P. J., and D. S. Schimel.
25. Remotely sensed temperature/vegetation index measurements for the purpose of assessing land surface moisture conditions The basic biosphere model is used for this investigation. Yongkang Xue, Kevin P. Czajkowski, and Samuel N. Gowarda. 2002, Vol. 79, Issue 2 (pp. 225-242), *Remote Sensing of Environment*.
26. Remote sensing of irrigated croplands: a simple algorithm 24. Two names to remember: Weicheng Wu and Eddy De Pauw. Global Institute of Sustainable Agriculture (ICARDA) at Great Basin International Studies University.
27. The use of remote sensing to create a map of the urban heat island phenomena. Asmala bin Ahmad, Noorazuan bin Md. Hashim, and Mardina binti Abdullah. Volume 68, Issue 3 (2007), *The Institution of Engineers, Malaysia*.
28. 26. USING LANDSAT ETM+ IMAGES TO ESTIMATE LAND SURFACE TEMPERATURE FOR RESEARCHING THE URBAN HEAT ISLAND EFFECT. K. SUNDARA KUMAR, P. UDAYA BHASKAR, and K. PADMAKUMARI, all of them are doctors. Volume 4, Issue 2 of the *International Journal of Engineering Science and Technology*, 2012.
29. DINDIGUL DISTRICT LAND SURFACE TEMPERATURE ESTIMATES FROM LANDSAT 8 IMAGES 27. *International Journal of Engineering and Technology*, Volume 3, Issue 5, 2014, Rajeshwari A. and Mani N. D.
30. Using LANDSAT TM-5 to retrieve surface temperatures, by Jose A. Sobrino, Juan C. Jimenez-Munoz, and Leonardo Paolini. *Remote Sensing of Environment*, Volume 90, Issue 4, Pages 434-440, 2004.
31. Mesoscale weather prediction using parameterization approaches for land-surface processes. *Evaporation from the Land's Surface*. 93-120 in Bougeault, P. (1991), Springer-Verlang, New York.
32. 30. Monitoring irrigation by keeping tabs on water levels using NOAA-AVHRR thermal infrared data. 1990, *IEEE Transactions on Geoscience and Remote Sensing*, vol. 28, pp. 949-954; Vidal, A.; Perrier, A.
33. Climates in Central North Carolina's Urban Core Studied Along the I-85/I-40 Corridor, Entry No. 31. CHARLES WATSON (Ph.D.) 2012.